Volcanic stratigraphy and mineralisation of the Archean Colomb-Chaboullié greenstone belt, James Bay, Québec, Canada

Sarah Galloway, Pierre-Simon Ross (INRS-Centre Eau Terre et Environnement, Québec), Daniel Bandyayera and Yannick Daoudene (Ministère de l'Énergie et des Ressources naturelles, Québec)

Abstract

The small Archean Colomb-Chaboullié greenstone belt, contains a series of base and precious metal-bearing sulphide prospects that indicate exploration potential in the area. Within this belt, sulphide mineralisation occurs as massive and semi-massive bodies dominantly located in the volcanic units, and as disseminated sulphide zones infilling the inter-pillow basalt material of the pillowed facies. Sulphide veins also occur in massive basalt flows, infilling fractures. Geochemical analysis will help increase the stratigraphic knowledge of this study area and perhaps help link the mineralisation with specific chemo-stratigraphic units. This study will help future exploration of greenstone belts in the northern region of the Superior Province that are underexplored in comparison to the Abitibi greenstone belt.

Location Map

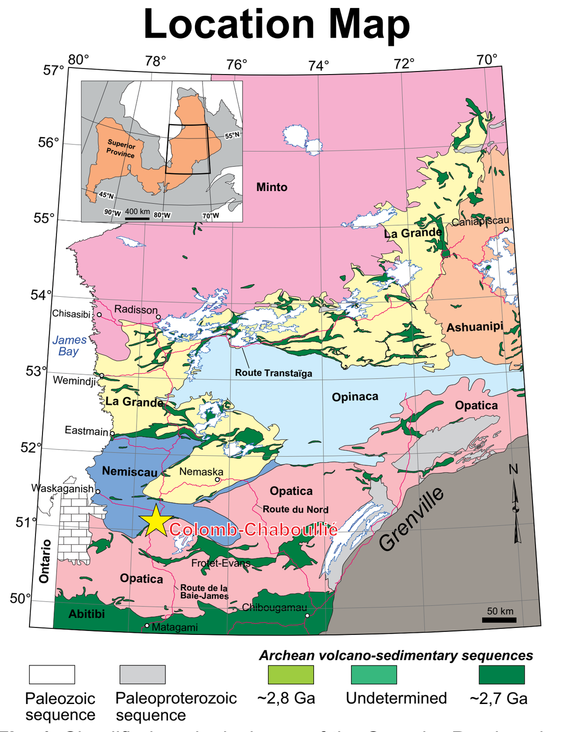

Fig. 1. Simplified geological map of the Superior Province in the James Bay region of Québec, showing the location of the Colomb-Chaboullié greenstone belt, after Bandyayera and Daoudene (in preparation).

Petrography

Fig. 2. Deformed pillows in basalt.

Fig. 4. Pillowed andesite.

Fig. 6. Laminations or schistosity in the felsic volcaniclastic unit.

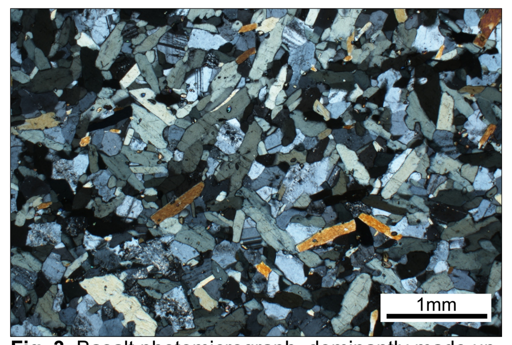

Fig. 3. Basalt photomicrograph, dominantly made up of amphiboles with plagioclase crystals.

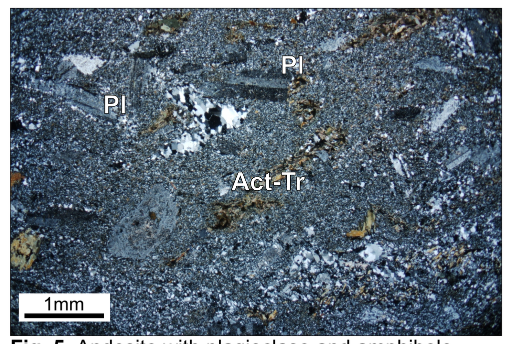

Fig. 5. Andesite with plagioclase and amphibole phenocrysts in a plagioclase-quartz rich matrix.

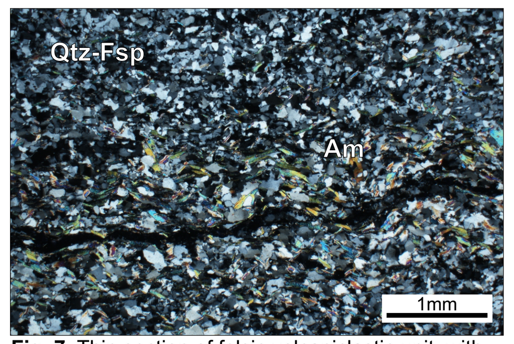

Fig. 7. Thin section of felsic volcaniclastic unit, with lamination/schistosity.

Mineralisation

Fig. 8. Deformed pillows in basalt with rusted inter-pillow material.

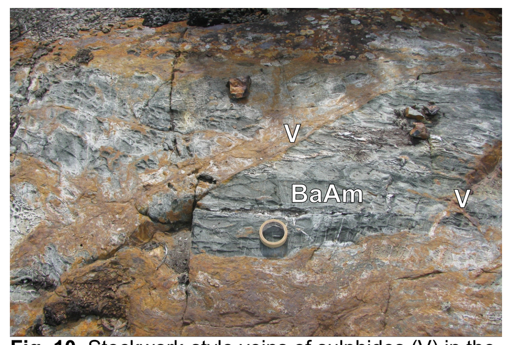

Fig. 10. Stockwork-style veins of sulphides (V) in the amphibolised basalt (BaAm).

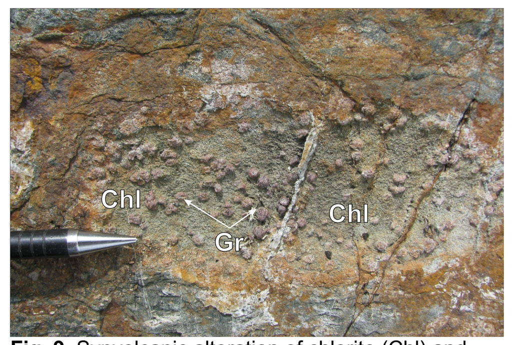

Fig. 9. Synvolcanic alteration of chlorite (Chl) and garnet (Gr) in the basalt pillow margins.

Fig. 11. Massive sulphide lens from the Lac Marcaut outcrop (16-SG-3521) containing gold values.

Massive Sulphides

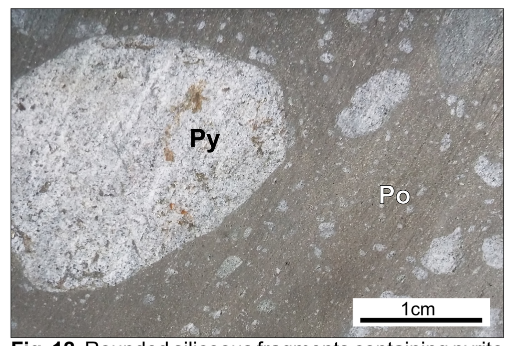

Fig. 12. Rounded siliceous fragments containing pyrite (Py) embedded in a pyrrhotite (Po) matrix.

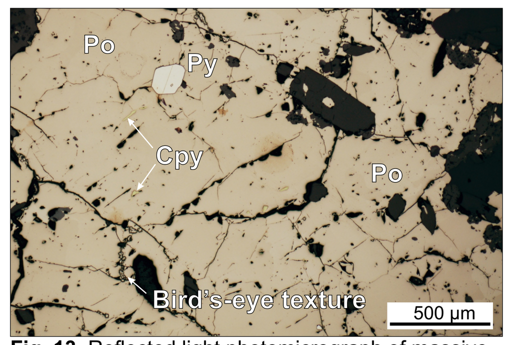

Fig. 13. Reflected light photomicrograph of massive sulphides from the Lac Marcaut outcrop.

Geological Map of the Colomb-Chaboullié Greenstone Belt

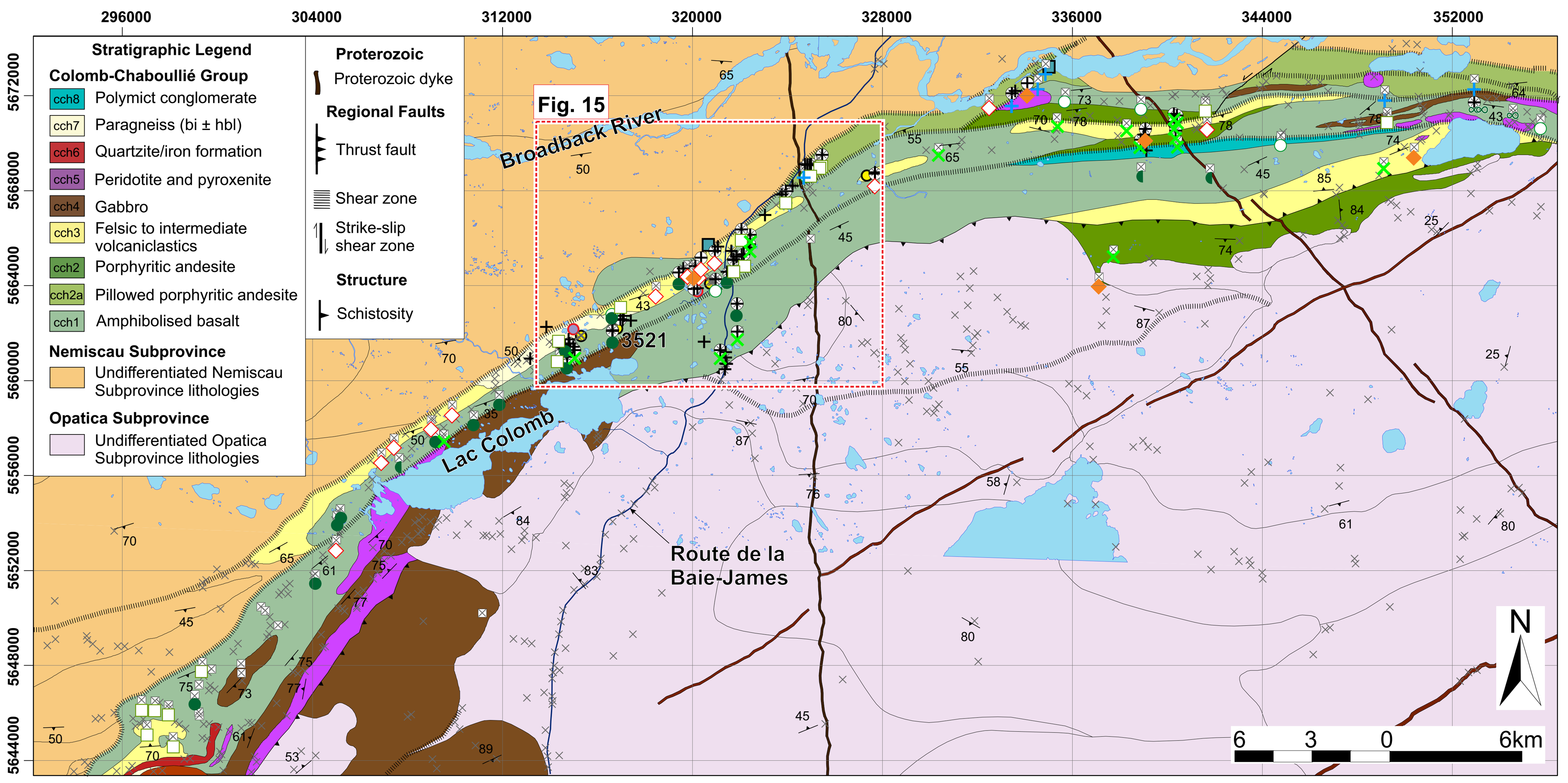

Fig. 14. Geological map of the Colomb-Chaboullié greenstone belt (after Bandyayera and Daoudene, 2015) showing the location of the outcrops mapped in 2016 by the first author, the outcrops mapped in 2015 by the MERN, the location of the 2016 and 2015 lithogeochemical samples, the locations of previously recorded mineralisation in the study area, and the stratigraphic placement of the geochemical units. See legend below in Geochemistry of the Colomb-Chaboullié Volcanic Units for details.

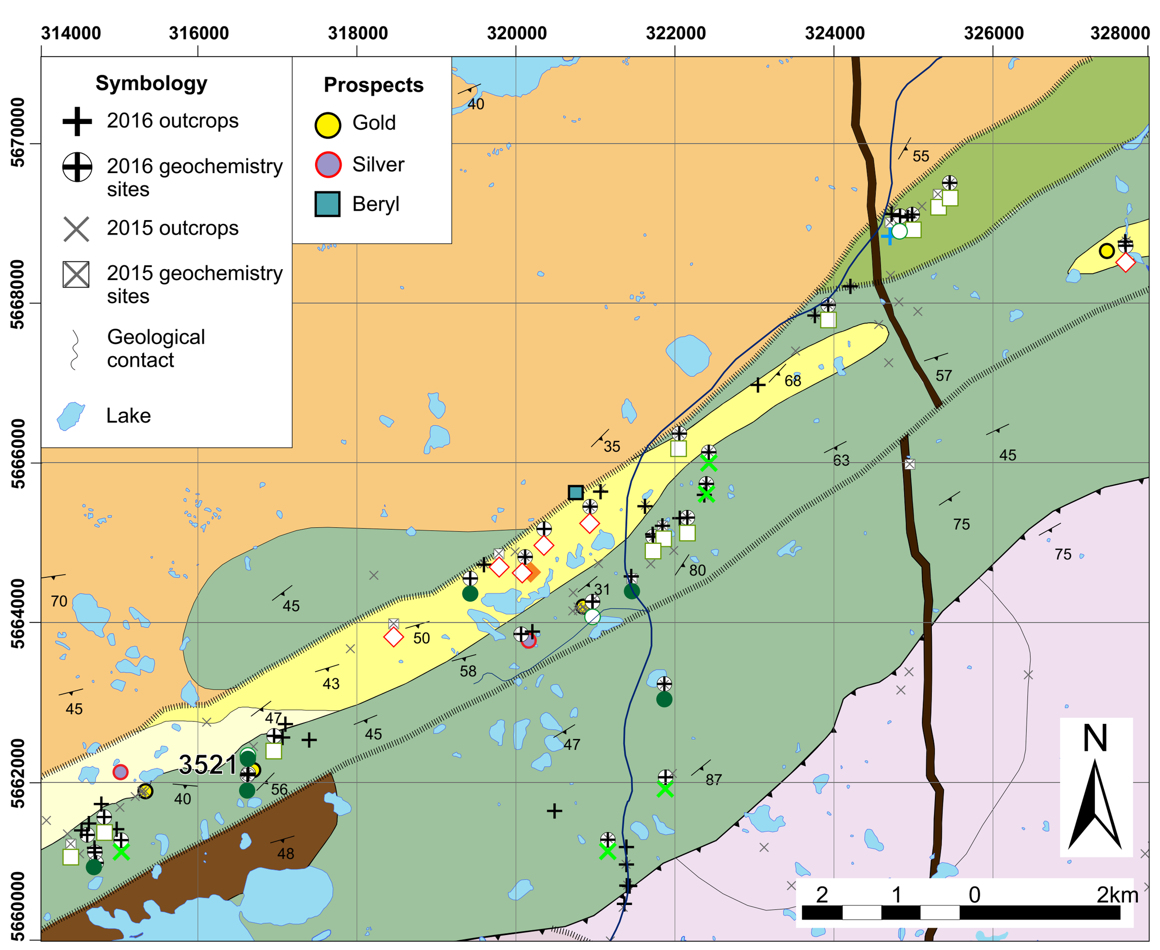

Fig. 15. Zoomed map of the main N-S transect through the volcanic units of the Colomb-Chaboullié belt, carried out by the first and second authors, showing the geochemical units. See legend below in Geochemistry of the Colomb-Chaboullié Volcanic Units for details.

Detailed Map of Outcrop 16-SG-3521

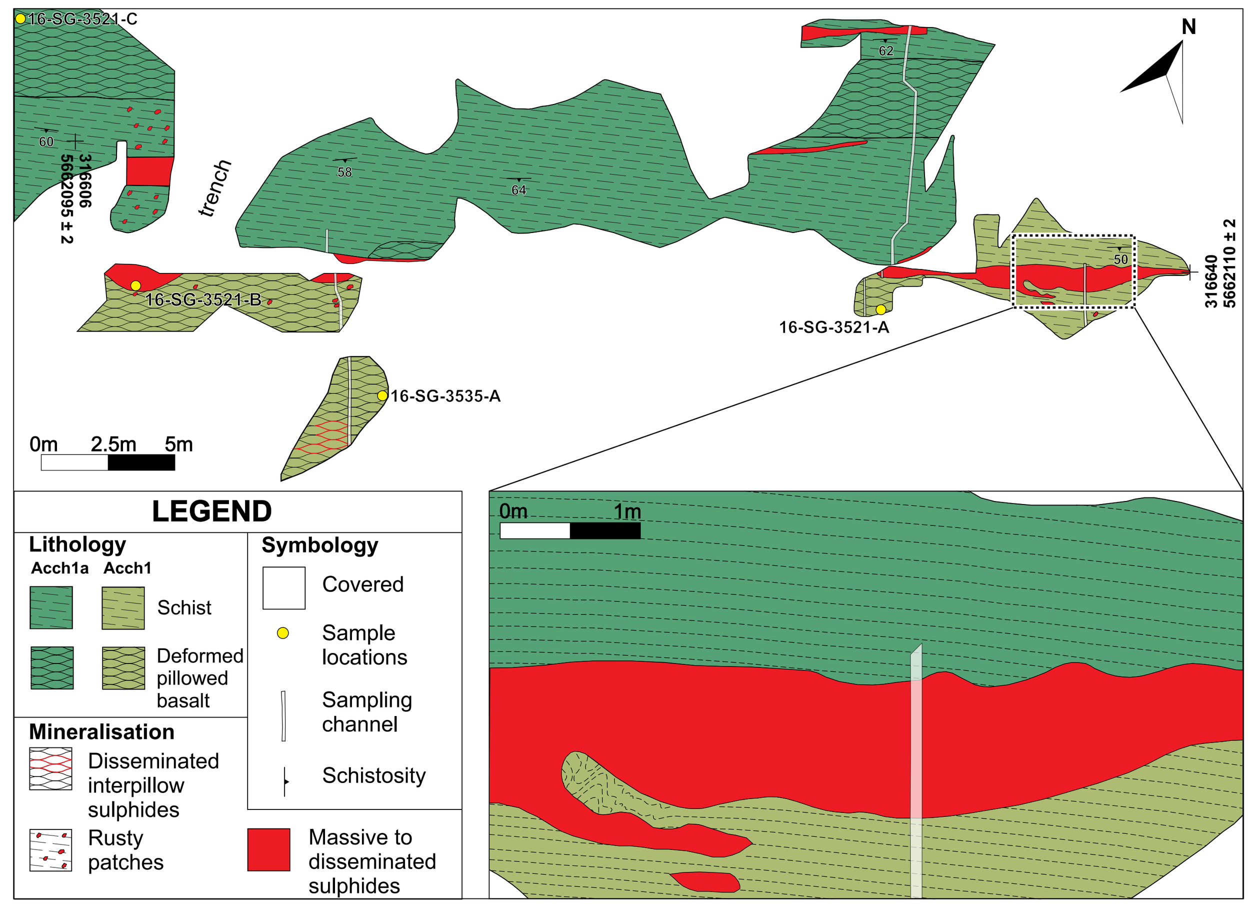

Fig. 16. This map illustrates the principle facies and the location of the disseminated and massive sulphide showings within this outcrop. Fig. 11 shows the sulphide lens in this outcrop orientated SW-NE, with the schistosity of the host rock cross cutting the sulphide lens.

Geochemistry of the Colomb-Chaboullié Volcanic Units

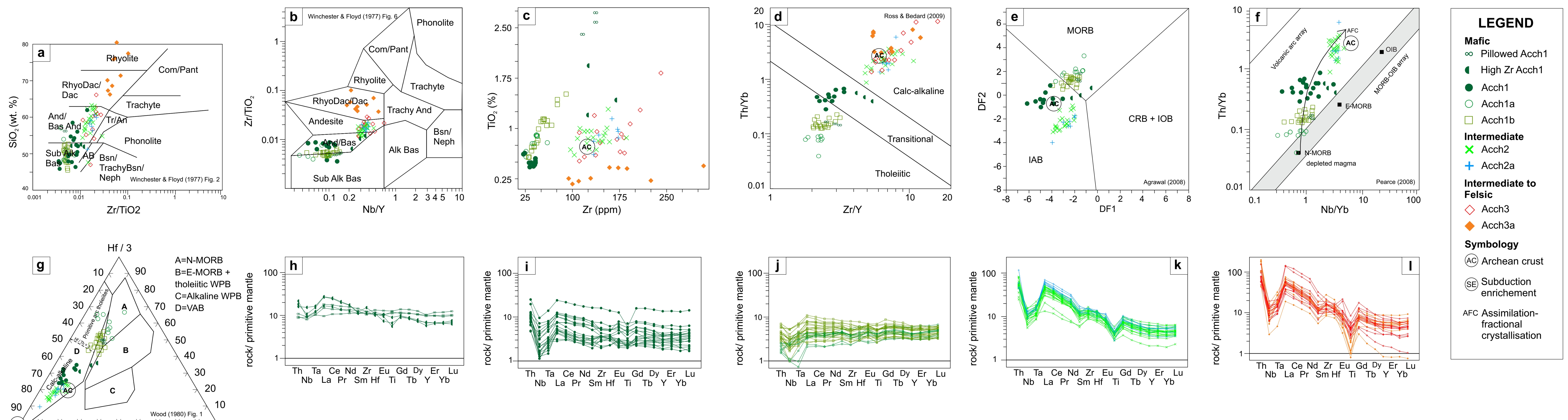

Fig. 17. Geochemical plots for the mafic to felsic volcanic rocks of the Colomb-Chaboullié greenstone belt. The amphibolised basalt has been divided into 3 main units (Acch1, Acch1a and Acch1b), with two smaller geochemical groups that define a basaltic unit in the east of the belt with well developed pillows, and the other unit defined by high Zr values. The Acch2 and Acch2a units are intermediate in nature, with Acch3 also showing similar characteristics to these intermediate groups. Acch3a represents the true felsic volcanic rocks within the Colomb-Chaboullié belt. The normalisation values for rare earth elements for the spider diagrams are after Sun and McDonough (1989).

Conclusions

The amphibolised basalt and andesite flows were deposited in a submarine setting which is evident by the presence of the pillowed facies in both of these lithologies (Figs. 2 and 4).

Disseminated sulphides were identified in both massive and pillowed basalt facies. In the pillowed flows, these sulphides were dominantly present in the interpillow material, often associated with chlorite and garnet (<5 mm) in the pillow margins (Fig. 9). This suggests that hydrothermal alteration and mineralisation occurred early on in the primary porosity between the pillows, before diagenesis, and is therefore synvolcanic. In the massive flows, the disseminated sulphides are facture-controlled and form a network of infilling fractures (Fig. 10). This stockwork fracture pattern of sulphides with chloritisation is typical of VMS-type mineralisation which also indicates that these sulphides are synvolcanic.

The geochemistry shows that these volcanic rocks span a range from sub-alkaline basalts to rhyodacite/rhyolite (Fig. 17a-b). The mafic groups (Acch1, Acch1a and Acch1b) are tholeiitic to transitional and plot in the MORB/IAB field (Fig. 17d-e). The intermediate units are calc-alkaline in composition and plot in the IAB field (Fig. 17d-e). The basalts originate from depleted magmas (N-MORB) and follow the AFC trend (Fig. 17f). The Archean crust interacts with these rocks during their evolution, however subduction enrichment may also play a part in the evolution of these rocks (Fig. 17g).

The basalts have a relatively flat REE profile with generally weak negative anomalies of Nb-Ta and Ti (Fig. 17h-j). The intermediate to felsic units are LREE enriched, with more pronounced Nb-Ta and Ti anomalies, suggesting magmatic differentiation and crustal contamination of the parent melt (Fig. 17k-l).

References

Agrawal S, Guevara M, Verma S (2008) Tectonic Discrimination of Basic and Ultrabasic Volcanic Rocks through Log-Transformed Ratios of Immobile Trace Elements. International Geology Reviews 50:1057-1079.

Bandyayera D, Daoudene Y (in preparation) Géologie de la région du lac Nemiscau, secteur du lac Royayer (SNRC 32K13, 32K14, 32N03 et 32N04-SE). MERN report.

Bandyayera D, Daoudene Y (2015) Géologie de la région du lac Nemiscau, secteur du lac Royayer, MERN. CG-2015-05. Carte 1:50,000

Pearce JA (2008) Geochemical fingerprinting of oceanic basalts with applications to ophiolite classification and the search for Archean oceanic crust. Lithos 100:14-48.

Ross P-S, Bédard JH (2009) Magmatic affinity of modern and ancient subalkaline volcanic rocks determined from trace-element discriminant diagrams. Canadian Journal of Earth Sciences 46:823-839.

Sun S-S, McDonough WF (1989) Chemical and isotopic systematics of oceanic basalts: implications for mantle composition and processes, in Saunders AD, and Norry MJ eds, Magmatism in the ocean basins. Geological Society Special Publication 42:313-345.

Winchester JA, Floyd PA (1977) Geochemical Discrimination of Different Magma Series and their Differentiation Products using Immobile Elements. Chemical Geology 20:325-343.

Wood DA (1980) The application of a Th-Hf-Ta diagram to problems of tectonomagmatic classification and to establishing the nature of crustal contamination of basaltic lavas of the British Tertiary volcanic province. Earth and Planetary Science Letters 50:11-30.